Chemical Engineering Journal 443 (2022) 136271

Contents lists available at ScienceDirect

Chemical Engineering Journal

journal homepage: www.elsevier.com/locate/cej

Moisture effect on the separation of CO_2/CH_4 mixtures with amine-functionalised porous silicas

Marlene Pacheco [a], Marta Bordonhos [a], Mariana Sardo [b], Rui Afonso [b], José R. B. Gomes [b], Luís Mafra [b], Moisés L. Pinto [a,*]

[a] CERENA, Instituto Superior Técnico, Universidade de Lisboa, Av. Rovisco Pais, n° 1, 1049-001 Lisboa, Portugal
[b] CICECO - Aveiro Institute of Materials, Department of Chemistry, University of Aveiro, Campus Universitário de Santiago, 3810-193 Aveiro, Portugal

ARTICLE INFO

Keywords:
Methane upgrading
Gas separation
Amine-functionalised silicas
Solid-state NMR
DFT computer simulations
Adsorption

ABSTRACT

The effect of minor amounts of water on the CO_2 and CH_4 adsorption on primary and secondary amine-functionalised mesoporous silicas (APTES@SBA-15 and DEAPTES@SBA15, respectively) was studied with a combination of high-pressure gas adsorption, solid state NMR of labelled $^{13}CO_2$ and density functional theory (DFT) calculations. Known amounts of water were pre-adsorbed on the materials (0.047 to 0.157 mmol•g^{-1}) and the adsorption performance for CO_2 and CH_4 was compared to the performance of the dry samples. We observed that even when only minor amounts of water are present, the tertiary amine-functionalised material revealed a significant enhancement of the selectivity for CO_2 (from *ca.* 5.8 to 208) while the one with primary amine maintained the same adsorption properties. This is related to the change in the adsorption mechanism in DEAPTES@SBA15 when water is present since water participates in the reaction of the tertiary amine with CO_2 to produce bicarbonate (confirmed by NMR and DFT results). Such species was not observed in APTES@SBA-15 with water. From a broader perspective, the results presented in this work are relevant to confirm the suitability of this type of hybrid adsorbents in industrial applications related with CO_2 adsorption, where minor amounts of water may be present in the process streams, such as during bio, landfill, or natural gas upgrading, or also in carbon capture applications.

1. Introduction

In the search for alternative energy sources, the exploitation of biogas and landfill gas sources that are rich in methane (CH_4) assume a relevant role in the reduction of the carbon footprint of modern societies. These gas sources are usually contaminated with a significant amount of carbon dioxide (CO_2) (<50 %) that needs to be removed to obtain fuel-grade methane (methane upgrading). Other contaminants are also present but their amounts rarely ascend to 1–5% [1]. Therefore, CO_2 and CH_4 are the main components in these mixtures that need to be separated. Indeed, the technologies to separate CO_2 from streams that contain a significant concentration of this gas need to be energy efficient, otherwise the trade-off for the purification of the biogas and landfill gas sources may be compromised, *i.e.*, the balance between the energy resulting from the obtained upgraded methane and the energy spent in the purification. Gas scrubbing with aqueous amine solutions is a commonly used technology for the removal of CO_2 from gaseous streams. However, this technology is energetically demanding due to the high temperature needed for regeneration (≈ 150 °C). Amine deactivation, toxicity and corrosion are also factors that make this process unsustainable in the long term. Thus, in the last decades, new alternatives are being considered to increase the energy efficiency of this purification step [2,3].

Adsorption by porous solids is an interesting alternative for the separation of gases, particularly of light gases that are close or above the critical point at ambient temperature [4]. In these cases, separation by distillation is usually avoided since it requires cryogenic conditions with high expenditures with several compression-cooling cycles to liquify the process stream, thus not being a viable alternative to the amine scrubbing process. The selective adsorption of one compound at the surface of a judiciously chosen solid adsorbent may be exploited to purify gas streams by separation processes. These processes are usually designed to be cyclic, with a step for the desorption of the most abundant gas thus allowing the regeneration of the adsorbent material to be used for

* Corresponding author.
E-mail addresses: ruivafonso@gmail.com (R. Afonso), moises.pinto@tecnico.ulisboa.pt (M.L. Pinto).

https://doi.org/10.1016/j.cej.2022.136271
Received 25 January 2022; Received in revised form 31 March 2022; Accepted 5 April 2022
Available online 7 April 2022

several cycles. In this context, it is extremely relevant to understand the effect of trace compounds occurring in the mixture that may accumulate in the adsorbent and change the adsorption behaviour for the main compounds to be separated. Natural and biogas sources are often contaminated with water that can be removed before the last step of methane purification to avoid problems during the processing of the gas mixture. Nevertheless, some trace amounts of water can still be present during the CH_4/CO_2 separation. If it is strongly adsorbed, this water can accumulate inside the adsorbent material and significantly change the adsorption behaviour. In the present work, we focus on the influence of moisture on the adsorption and separation of CO_2 and CH_4, using amine-functionalised mesoporous silicas.

Mesoporous silicas functionalised with amines are a type of hybrid adsorbent material that have been extensively explored as adsorbents to capture CO_2 from flue gases, for eventual application in carbon capture technologies [5]. Impregnation of the pores with amine containing polymers or grafting amine groups at the surface of the pores are the two main routes to produce aminated materials with high selectivity and capacity towards CO_2 at low partial pressures [6]. Mesoporous silicas with wide pores, like SBA-15, are normally chosen to be easily functionalised with high amounts of covalently tethered amines. These materials can capture CO_2 from flue gas even in the presence of moisture [7–9]. Our team has previously demonstrated that this type of materials can be efficiently used for the separation of CO_2 from CH_4, particularly when primary amines are used [10]. With this type of amines, the materials can be partially regenerated in pressure swing cycles at ambient pressure or using moderate vacuum, affording an interesting working capacity while exhibiting excellent selectivity towards CO_2. This happens because CO_2 is chemisorbed and the species formed at the surface of the material are stabilised by a network of hydrogen bonds. Nevertheless, they still remain labile and the equilibrium can be displaced to obtain again CO_2 by vacuum [11]. After the saturation of the amine layer with CO_2, yielding different types of hydrogen-bonded carbamic acid species at the surface, the CO_2 continues to be selectively adsorbed over CH_4 due to the polarity of the species formed at the surface extending the high selectivity of these materials to pressures above the atmospheric one [10]. Thus, these materials present interesting properties for CO_2/CH_4 separation over a large range of pressures making them attractive for cyclic processes with pressure swing adsorption – PSA.

More recently, we explored the effect of small amounts of water on the speciation of the chemisorbed CO_2 at the surface of the amine-functionalised mesoporous silicas [12]. In the adsorbent materials functionalised with neighbouring primary amines, the water promotes the proton transfer of carbamic acid to nearest-neighbouring amines, leading to formation of alkylammonium carbamate ion pairs, while in materials with isolated amines the acidic proton of the carbamic acid is transferred to a water molecule. Interestingly, tertiary amines displayed an enhanced interaction with CO_2 in the presence of water, but in this condition the adsorption occurs via the formation of bicarbonates since there are no protons on the amines that can be transferred to CO_2. In the present work, we explore how the presence of small amounts of water at the surface of primary and tertiary amines changes the adsorption properties for CO_2 and CH_4, and how it influences the separation of these gases. A combination of adsorption experiments in dry and wet samples with information from solid state NMR and electronic density functional theory models afforded a molecular level interpretation of the observed changes in CO_2/CH_4 selectivity.

2. Methods

2.1. Materials synthesis

SBA-15 (7 nm pore size) was purchased from Sigma-Aldrich. SBA-15 was functionalised with amino-organosilanes; amino-propyltriethoxysilane – APTES (purity greater than 98%; Sigma-Aldrich) and 3-(diethylamino)propyltrimethoxysilane – 3-DEAPTES (96%; Sigma-Aldrich). To ensure the dryness conditions of the reaction media and material to prevent silane polymerisation within, 2 g of SBA-15 was introduced in a closed reflux apparatus connected to a vacuum line and heated to 150 °C for 2 h. After cooling, nitrogen was introduced into the system prior to the opening of the reflux apparatus, and SBA-15 was refluxed with 100 cm^3 of dry toluene (99.8%; Sigma-Aldrich) containing 9 mmol of the amino-organosilane for 24 h in a nitrogen atmosphere. The resulting material was purified by Soxhlet extraction with dry toluene, to remove the unreacted amino-organosilanes, and finally dried under vacuum at 120 °C for 24 h. Functionalised materials were named APTES@SBA-15 and DEAPTES@SBA-15.

2.2. Materials characterisation

The porosity of the materials was determined by nitrogen (N_2) adsorption at −196 °C. The N_2 adsorption isotherms were obtained in an automatic apparatus, Micromeritics ASAP 2010. Prior to isotherm measurement, the samples (~ 50 mg) were outgassed at 150 °C under vacuum greater than 10^{-2} Pa, for 2.5 h. From N_2 adsorption data, the specific surface area (A_{BET}) was determined through Brunauer-Emmett-Teller (BET) equation in the $0.05 < p/p^0 < 0.2$ pressure range [13], and the total pore volume (V_{pore}) was assessed by the Gurvich rule [13], corresponding to the volume of N_2 adsorbed at $p/p^0 = 0.95$. The mesopore size distributions were obtained by the Broekhoff-de Boer (BdB) method, in a version simplified with the Frenkel-Halsey-Hill (FHH) equation [14] that was previously shown to give accurate results when applied to mesoporous silicas and silicates [15].

Elemental analysis was performed on a Truspec 630–200-200 equipment, using thermal conductivity as the detection method for nitrogen (combustion temperature of 1075 °C). The thermogravimetric, differential scanning calorimetry experiments was performed using the same protocol as described in our previous work [11] (details in the Supporting Information).

2.3. Adsorption of carbon dioxide and methane above atmospheric pressure

The CO_2 (99.998%; Air Liquide) and CH_4 (99.995%; Air Liquide) adsorption isotherms were collected at 25 °C in increasing pressures up to ca. 1000 kPa (10 bar), using the manometric method, in a lab-made stainless-steel volumetric apparatus [16] with a pressure transducer (MKS, Baratron 627D14TBC1B), and equipped with a vacuum system (Pfeiffer Vacuum, HiCube 80 Eco). Prior to collecting experimental data, all samples were degassed at 150 °C for 2 h, under a vacuum pressure of 10^{-4} Pa. During the experiments, the temperature of the adsorption system and of each sample was controlled with a thermostatic water bath with an accuracy of 0.01 °C (Julabo, MB-5). Experimental adsorption isotherms were obtained considering the non-ideality of the gas phase using the second and third virial coefficients. Excess adsorbed amounts were converted to the absolute adsorbed amounts considering the porous volume of the material and the density of the gas phase [17]. The average selectivity and phase diagrams of binary CO_2/CH_4 mixtures were estimated by a method proposed by Myers [18] based on the Ideal Adsorbed Solution Theory (IAST) [19]. The implementation of this method requires the use of an analytical expression to fit the experimental adsorption equilibrium isotherms that, in the scope of this work, is given in the form of a Langmuir-virial equation (1) for the adsorption of CO_2, and a virial equation (2) for the adsorption of CH_4, in which the pressure, p, is a function of the adsorbed amount, n^{ads}, as follows:

$$p = \frac{n^{ads}}{K} \bullet \frac{m}{m - n^{ads}} \exp\left(C_1 n^{ads} + C_2 n^{ads^2} + \cdots\right) \quad (1)$$

$$p = \frac{n^{ads}}{K} \exp\left(C_1 n^{ads} + C_2 n^{ads^2} + \cdots\right) \quad (2)$$

and where K is the Henry constant, m is the saturation capacity and (C_1, C_2, …) are the respective coefficients of the virial series expansion needed to fit the experimental data points [18]. A detailed description of the complete implementation of this method can be found in previous works [20,21].

To study the effect of the presence of a small amount of adsorbed water on the adsorption of CO_2 and CH_4, a given pressure of water vapour was introduced in the calibrated volume (up to *ca.* 2.1 kPa) and then dosed to the freshly activated sample. After equilibrium, the final pressure was below the sensitivity of the pressure transducer (<6 Pa) and it was assumed that all the amount of water was adsorbed in the sample. For the calculations of the amounts adsorbed, the non-ideality of the water vapour was accounted with the second viral coefficient. Prior to use, deionised water (Millipore Milli-Q) was further purified by freeze – vacuum – thaw cycles.

2.4. Solid-state NMR measurements

^{13}C solid-state (ss) NMR spectra were acquired on a Bruker Avance III 700 spectrometer operating at $B_0 = 16.4$ T, with ^{13}C Larmor frequency of 176.1 MHz. All experiments were performed on a double-resonance 4 mm Bruker MAS probe and the samples were packed into ZrO_2 rotors with Kel-F caps with a spinning rate of 12 kHz. ^{13}C CSs are quoted in ppm from α-glycine (secondary reference, carbonyl peak at 176.03 ppm). The ^{13}C CPMAS spectra were acquired under the following experimental conditions: ^{1}H 90° pulse set to 3.0 μs corresponding to a rf of ~83 kHz; the CP step was performed with a contact time (CT) of 2000 μs using a 70–100% RAMP shape at the ^{1}H channel and using a 50 kHz square shape pulse on the ^{13}C channel; RD was 5 s. During the acquisition, a SPINAL-64 decoupling scheme was employed using a pulse length for the basic decoupling units of 7 μs at rf field strength of 83 kHz.

2.5. Computational details

The electronic density functional theory calculations considered the M06-2X functional [22,23] and the 6-31G(d) basis set [24,25], and were performed with the Gaussian 09 package [26]. This combination of exchange–correlation functional and basis set was found to be adequate for geometry optimisation and calculation of ^{1}H, ^{13}C and ^{15}N NMR shifts [11,12,27] with the GIAO method [28,29], yielding accuracies similar or even better than those obtained with computationally more expensive approaches [12].

The molecular models were obtained as in our previous studies [11,12,27], *i.e.*, upon replacing three surface OH groups with silylpropylamines on the surface of molecular clusters cut from the periodic experimental crystallographic structure of alpha-quartz, and with dangling bonds at the edges of the cluster models due to elimination of Si atoms saturated with H atoms along the O–Si directions.

3. Results and discussion

3.1. Characterisation of the adsorbent materials

The present work is focused on the influence of pre-adsorbed water for CO_2/CH_4 separation. Besides the effect of amine functionalisation, gas separation may also be affected by the textural properties of the samples. The functionalisation affected the pore size distribution and respective N_2 adsorption isotherms of the samples (Fig. 1). The textural properties and the nitrogen (N) content are listed in Table 1. Successful amine functionalisation can be inferred from the decrease of BET surface area from *ca.* 743 (parent SBA-15) to 340 and 329 $m^2 \bullet g^{-1}$ upon functionalisation with APTES and DEAPTES, respectively. The pore volume has also decreased upon functionalisation with both amines, with a slightly higher decrease for the material functionalised with the bulkier DEAPTES amine. No significant change was observed on the pore

Table 1
Textural properties determined from N_2 adsorption/desorption isotherms at −196 °C and N content obtained from elemental analysis of the amine-functionalised SBA-15 materials.

Material	A_{BET} [a] $m^2 \bullet g^{-1}$	V_{pore} [b] $cm^3 \bullet g^{-1}$	d_{pore} [c] nm	N content [d] $mmol \bullet g^{-1}$
SBA-15	743 ± 3	0.839	7.0	—
APTES@SBA-15	340 ± 2	0.665	7.8	1.08
DEAPTES@SBA-15	329 ± 3	0.585	7.0	1.00

[a] Specific surface area (A_{BET}) calculated by the BET equation; [b] Total porous volume (V_{pore}) calculated from the adsorbed amount at $p/p^0 = 0.95$ [13]; [c] Maxima of the pore size distributions (d_{pore}) shown in Fig. 1; [d] N content determined by thermogravimetry with differential scanning calorimetry in ref. [11].

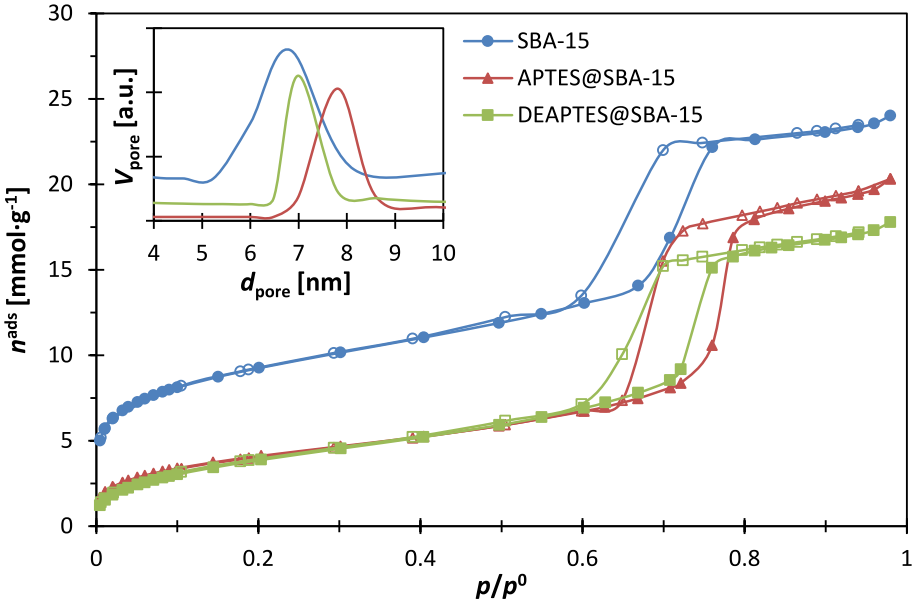

Fig. 1. N_2 adsorption (closed symbols) and desorption (open symbols) isotherms at −196 °C, and pore size distribution for SBA-15 (blue circles), APTES@SBA-15 (red triangles) and DEAPTES@SBA-15 (green squares). Note: pore size distributions obtained from the BdB-FHH method [14].

diameter, although a minor difference can be noticed from APTES@SBA-15 to SBA-15 that may be attributed to variations in SBA-15 batch synthesis. The N content determined on both functionalised samples, 1.08 mmol•g^{-1} for APTES@SBA-15 and 1.0 mmol•g^{-1} for DEAPTES@SBA-15 and the FTIR/ssNMR measurements, further supports a successful functionalisation of the materials.

The infrared spectra (Figure S1) of the functionalised materials display additional vibrations in the region of 3500–3300 cm^{-1} (stretching of N–H bond) and 1650–1580 cm^{-1} (N–H amine bending). The ^{13}C ssNMR spectra of APTES@SBA-15 and DEAPTES@SBA-15 (Figure S2) exhibit three resonances (8.7, 21.5 and 42.5 ppm) corresponding to the propyl chain and four resonances (9.6, 19.4, 46.2 and 56.7 ppm) corresponding to the propyl chain and ethyl groups, respectively. A more detailed discussion of the characterisation of the samples can be found in our previous works [11,12].

3.2. Adsorption of carbon dioxide and methane under dry and wet conditions

The CO_2 and CH_4 adsorption equilibrium isotherms at 25 °C and for pressures up to 1000 kPa (10 bar) obtained for the two amine-functionalised SBA-15 materials under dry and wet conditions can be found in Fig. 2. The two studied materials (under dry and wet conditions) show a significantly greater affinity towards CO_2 than CH_4, which is a good indicator of the materials' potential for the separation of these two gases. The results confirm that the functionalisation with amines selectively enhances CO_2 adsorption particularly at low pressures when comparing with the parent SBA-15, in agreement with previous results [10]. Furthermore, the linear tendency of the CH_4 adsorption isotherms is representative of the low interaction of this gas with the pore surface of both materials. Considering the adsorption of CO_2 on the dry materials (Fig. 2, red triangles), APTES@SBA-15 shows a higher CO_2 uptake compared to DEAPTES@SBA-15. This is due to two effects. One is the bulkier nature of the tertiary amine which limits CO_2 adsorption. The second, and most important, is the types and strength of interactions of the primary amine with CO_2 [10–12,30].

When low amounts of water vapour were pre-adsorbed into the dry materials (section 2.3), the effect on the CO_2 and CH_4 adsorption is significantly different in both materials. We opted to use small amounts of water vapour because we were interested in studying the effect of minor amounts on the pore surface and not on the filling of the pores, when each gas is adsorbed.

For APTES@SBA-15, when *ca.* 0.157 mmol•g^{-1} of water vapour is loaded into the material prior to the CO_2 and CH_4 adsorption experiments, the change in the isotherms is not significant. Regarding CO_2 adsorption under wet conditions, the isotherm (Fig. 2a, purple squares) overlaps with the corresponding dry material adsorption isotherm (Fig. 2a, red triangles), indicating that, under such experimental conditions, a low amount of moisture on the surface does not enhance the CO_2 adsorption capacity. This is in contrast to what has been reported in the literature, where some studies [31–33] indicate that there is an increase in CO_2 adsorption capacity under wet conditions in silicas modified with primary amines, partly as a result of the formation of bicarbonate species that could, in theory, double the CO_2/N molar ratio from 0.5 (under dry conditions) to 1 (under wet conditions). However, our previous findings [12] have shown that bicarbonate species, if formed under wet conditions in primary-amine-modified materials, would not be present in a sufficiently high amount to justify an increase in CO_2 adsorption capacity.

For DEAPTES@SBA-15, the influence of water on the pore surface of the materials upon CO_2 adsorption was analysed using two different pre-adsorbed water vapour contents: *ca.* 0.140 mmol•g^{-1} (close to the value used on APTES@SBA-15) and *ca.* 0.045 mmol•g^{-1} (corresponding to *ca.* 2.1 and 0.7 kPa respectively). For the former, the amount of pre-adsorbed water is close to that used for the sample modified with the primary amine, and the main goal of this test was to compare the influence of a similar amount of pre-adsorbed water on the uptake of CO_2 on both materials. For the latter, the main goal was to see if such a low amount of pre-adsorbed water would lead to any change in CO_2 uptake on DEAPTES@SBA-15, and if so, to what extent.

For the test with the highest amount of pre-adsorbed water, 0.140 mmol•g^{-1}, there is a substantial increase in CO_2 uptake in comparison with the dry sample (Fig. 2b, purple squares and red triangles, respectively). In fact, the CO_2 uptake in the wet material is, on average, *ca.* twice as high as in the dry material, over the whole pressure range. This difference is even more significant at sub-atmospheric pressures (below *ca.* 100 kPa), presenting a 2.9-fold increase in CO_2 uptake in comparison with the dry material. At higher pressures, CO_2 uptake is approximately 1.2-times higher on the wet material. Using 0.045 mmol•g^{-1} of pre-adsorbed water is sufficient to increase the CO_2 uptake considerably (up to 1.7-fold) over the whole pressure range in the tertiary-amine-modified material (Fig. 2b, orange crosses). This significant increase in CO_2 uptake is attributed to the formation of bicarbonate species in the presence of water, as opposed to primary amine-modified materials [12]. DEAPTES@SBA-15 loaded with *ca.* 0.140 mmol•g^{-1} of pre-adsorbed water vapour shows ca. 1.3-fold increase in CO_2 uptake (up to 250 kPa) compared to APTES@SBA-15, either in dry or wet conditions. About the same trend is observed when loading *ca.* 0.045 mmol•g^{-1} of pre-adsorbed water vapour (up to *ca.* 130 kPa).

Regarding the adsorption of CH_4, the pre-adsorption of 0.133 mmol•g^{-1} of water vapour leads to a decrease in CH_4 uptake in comparison with the dry sample (Fig. 2b, green diamonds and blue circles, respectively). This effect can either be attributed to the presence of the pre-adsorbed water on the pore surface, leaving less space available for the already limited adsorption of CH_4 or to the decrease of CH_4 interactions with surface groups.

For a more quantitative analysis, the experimental results for CO_2 and CH_4 were fitted to the virial isotherm equations (1) and (2),

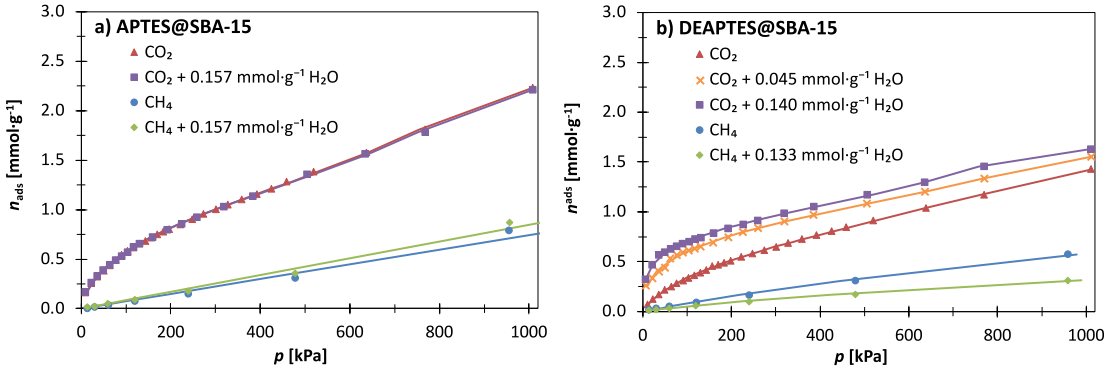

Fig. 2. Adsorption equilibrium isotherms of CO_2 and CH_4 at 25 °C obtained for the SBA-15 materials functionalised with the primary amine APTES (a) and tertiary amine DEAPTES (b) under dry and wet conditions. Solid lines represent the nonlinear least-squares fit of the Virial model to the experimental points (*cf.* Table 2).

respectively, as shown by the solid lines in Fig. 2, and the obtained parameters can be found in Table 2. As depicted in Table 2, the Henry constants (K) obtained for all CO_2 adsorption experiments are higher than those for CH_4, thus corroborating that both materials display higher affinity for the former than the latter in all situations studied. Under dry conditions, for APTES@SBA-15, Henry's constant for CO_2 is *ca.* 25 times higher than for CH_4, and under wet conditions no significant change in this ratio was observed, confirming the negligible effect of the pre-adsorption of water vapour on this material. For DEAPTES@SBA-15 under dry conditions, the value of K determined for CO_2 is only *ca.* 8 times higher than for the hydrocarbon. However, under wet conditions, Henry's constant for CO_2 adsorption becomes more than 1000 times higher than for CH_4 (for the highest moisture content), thus showing the overwhelmingly positive effect that the presence of pre-adsorbed water in the separation. Comparing only these quantitative adsorption results for CO_2 adsorption, it is also interesting to note that the Henry constant for APTES@SBA-15 is almost three times higher than for DEAPTES@SBA-15 under dry conditions. However, under wet conditions (highest amount of pre-adsorbed water), the value of K obtained for DEAPTES@SBA-15 is now 30 times higher than for APTES@SBA-15. The saturation capacity, m, obtained using the Langmuir-virial equation (2) to fit the CO_2 experimental adsorption data, is higher for APTES@SBA-15 than for DEAPTES@SBA-15 in all situations tested, and, for each material, decreases slightly with increasing content of pre-adsorbed water vapour. This was expected considering that the surface area and pore volume are higher for APTES@SBA-15, and that the pre-adsorbed water molecules leave less space available for the adsorption of the other molecules. Overall, APTES@SBA-15 shows a higher CO_2 uptake and saturation capacity. However, at low-pressures, where adsorption is mainly driven by interactions of the gases with the pore surface of the materials, the adsorption of CO_2 in DEAPTES@SBA-15 appears to improve considerably under wet conditions.

To summarise, the adsorption experiments have shown that both materials adsorb higher amounts of CO_2 than CH_4, demonstrating that the presence of a small amount of pre-adsorbed water vapour affects the adsorption of CO_2 on SBA-15 functionalised with primary and tertiary amines in completely opposite ways. In the primary-amine-modified SBA-15, the pre-adsorption of water vapour does not appear to have induced changes in the adsorption mechanism of CO_2 that would result in any significant difference in its uptake. In contrast, in SBA-15 functionalised with a tertiary amine, the pre-adsorption of water vapour induces a remarkable increase in CO_2 uptake, as a consequence of a significant change in the CO_2 adsorption mechanism, *i.e.*, the formation of bicarbonate species [12]. Before application of these materials in industrial systems for CO_2/CH_4 separation, the effect of the feed water concentration on the separation performance must be established. Nevertheless, our results clearly show that for amounts of accumulated water below $\sim$ 0.15 mmol•g^{-1} the effect is either null or positive for primary or tertiary amine functionalized materials, respectively.

3.3. Separation of carbon dioxide and methane mixtures

The variation of the average selectivity towards CO_2 with pressure for both materials under dry and wet conditions can be found in Figs. 3 and 4. For both materials under dry and wet conditions, the predicted average selectivity sharply increases in the lower-pressure region until it reaches a maximum around 134 kPa. After reaching the maximum, the selectivity of the separation decreases gradually with increasing pressures for all scenarios, until it begins to stabilise in the high-pressure region, *i.e.*, above 800–900 kPa. The initial sharp increase observed may be attributed to the concomitant effect of the strong chemical interactions between CO_2 and the different amine moieties (with or without pre-adsorbed water) and the CO_2 physisorption against the previously formed CO_2 chemisorbed species [10,11]. Above 134 kPa, as pressure continues to increase, this concomitant effect has a weaker expression and thus the selectivity decreases [10].

For the case of APTES@SBA-15, the pre-adsorption of water vapour could potentially have a slightly negative effect on the separation of a binary CO_2/CH_4 mixture above 134 kPa (*cf.* Fig. 3). However, for DEAPTES@SBA-15, the overwhelmingly positive effect that the pre-adsorption of water vapour could potentially have on the separation of CO_2/CH_4 gas mixtures is clear from the analysis of the average selectivity (*cf.* Fig. 4).

The significant increase in the CO_2/CH_4 selectivity of DEAPTES@SBA-15 due to the presence of water is consistent with the changes observed in the NMR spectra once dry and wet samples are exposed to ^{13}C-labelled CO_2 (Fig. 4). The presence of water in this sample promotes the formation of a CO_2 adduct at the surface with a chemical shift at ca. 161 ppm, while in the dry sample the observed resonance appears at ca. 155 ppm. The assignment of these resonances, assisted by DFT calculations (optimised molecular models and calculated chemical shifts in the insets of Fig. 4), indicates that the spectral changes arise from the formation of bicarbonate in the presence of water, not observed in dry conditions [12]. The pre-adsorbed water, allowing the formation of bicarbonate at the surface of the DEAPTES@SBA-15 material, promotes the CO_2 chemisorption that would be otherwise impossible, explaining the extraordinary increase in the selectivity for this gas in CO_2/CH_4 mixtures.

The spectra obtained for APTES@SBA-15 after $^{13}CO_2$ adsorption in the presence of water (Fig. 3) shows differences with respect to the dry sample, in particular the disappearance of the resonance at 154 ppm under moist conditions, consistent with our previous work [12]. The other important change is the area increase of the other bands observed at $\sim$ 160 and $\sim$ 164 ppm. These changes are due to an increase of the deshielding of the carbon of the carbonyl group and an increase in the charge separation between the amine and carbamic acid groups, but without the formation of bicarbonate. A complete discussion on the NMR and DFT results may be found in our recent work [12]. The main feature to highlight here is that the changes induced by the presence of water at the surface of the material functionalised with the primary amine do not significantly affect the selectivity for CO_2 in CO_2/CH_4

Table 2
Estimated Henry constants (K), saturation capacities (m) and virial coefficients (C_1, C_2) for the adsorption of CO_2 and CH_4 on the studied materials under dry and wet conditions.

Sample	Gas	$n_{H2O,pre\text{-}adsorbed}$ (mmol·g^{-1})	K (mol·kg^{-1}·kPa^{-1})	m (mol·kg^{-1})	C_1 (kg·mol^{-1})	C_2 (kg·mol^{-1})^2
APTES@SBA-15	CO_2	—	1.85×10^{-2}	2.61	2.15	–0.92
		0.157	1.96×10^{-2}	2.58	2.24	–0.96
	CH_4	—	7.44×10^{-4}	—	—	—
		0.157	8.46×10^{-4}	—	—	—
DEAPTES@SBA-15	CO_2	—	6.85×10^{-3}	1.89	1.94	–1.27
		0.045	9.80×10^{-2}	1.83	5.58	–2.65
		0.140	5.88×10^{-1}	1.79	8.22	–3.74
	CH_4	—	8.38×10^{-4}	—	0.62	—
		0.133	5.39×10^{-4}	—	1.70	—

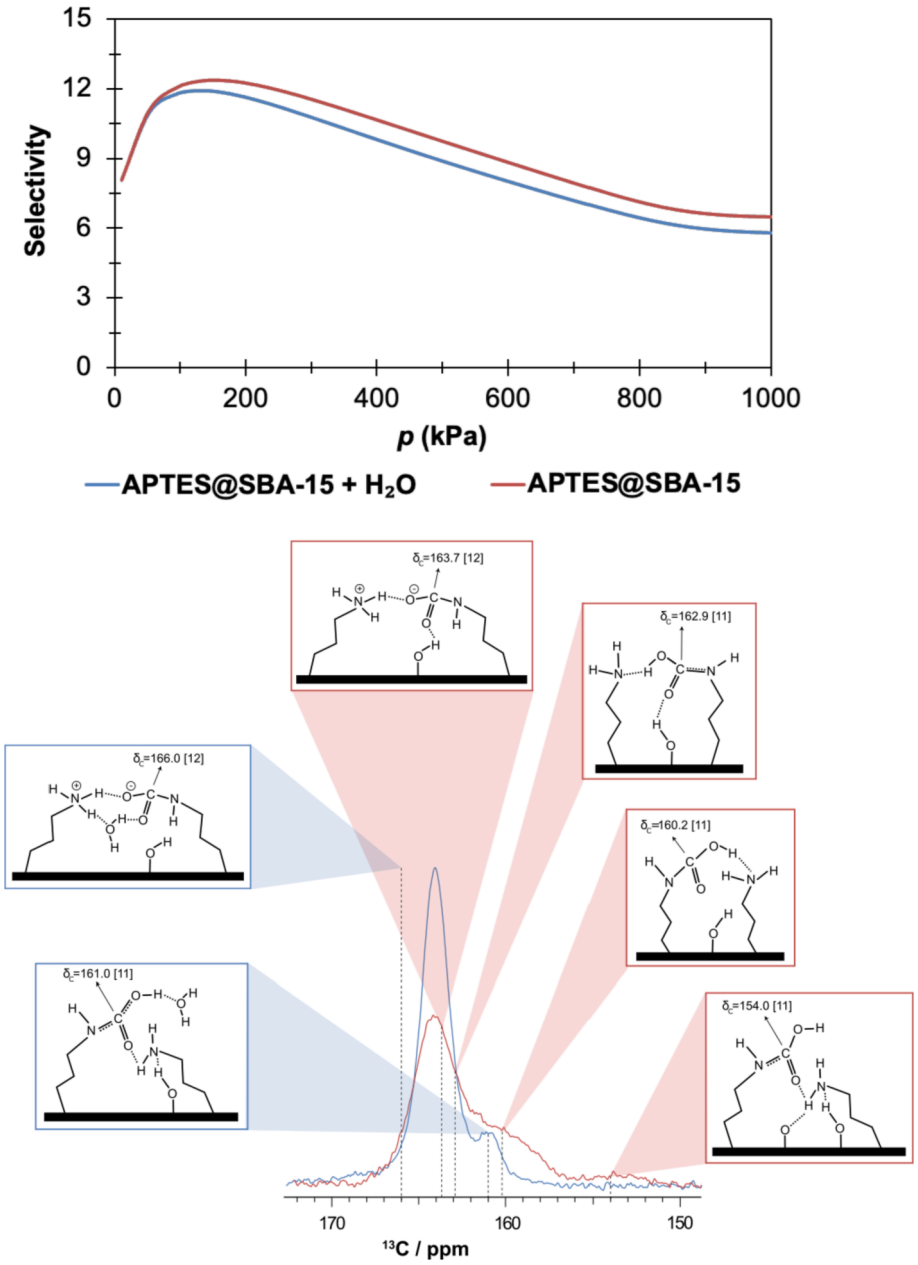

Fig. 3. Variation of the average selectivity towards CO_2 at 25 °C and up to 1000 kPa, and corresponding NMR spectra of samples with adsorbed $^{13}CO_2$ on APTES@SBA-15 under dry (red lines) and wet (blue lines) conditions. The assignment of the chemical shifts (in ppm) to the corresponding structures was assisted by DFT calculations on cluster models and the details are given in the references above the structures.

mixtures, in contrast with the observations made with the material functionalised with the tertiary amine.

The equilibrium phase diagrams (Fig. 5), further corroborate the main findings already presented in this study: under dry conditions, APTES@SBA-15 appears to have a higher affinity towards CO_2 than DEAPTES@SBA-15, whereas under wet conditions the latter appears to be more selective towards CO_2. As a practical example, considering an equimolar CO_2/CH_4 mixture ($y(CH_4) = 0.5$), the molar fraction of CO_2 in the adsorbed phase is *ca.* 89% and 88% for APTES@SBA-15 under dry and wet conditions, respectively (*cf.* Fig. 5a), and *ca.* 83% and 99% for DEAPTES@SBA-15 under dry and wet conditions, respectively (*cf.* Fig. 5b).

The Gibbs energy of the reaction (ΔG^{298}) of CO_2 with the surface amine groups, calculated using the same level of theory and the cluster models used to assist the chemical shifts assignment (Table 3), gives quantitative description on the effect of water in this reaction, namely on the equilibrium between the gas and adsorbed phase CO_2. In the case of primary amines (APTES@SBA-15), the reaction of CO_2 is already favourable without the presence of water, even with different amine environments and final CO_2 adducts (ΔG^{298} between −4.7 and −43.3 kJ•mol^{-1}, with negative values meaning exothermic reactions). In the presence of water, the calculations yielded lower ΔG^{298} values (more favourable reaction) for the comparable amine environments (*i.e.* same initial models in cf. Figs. 3 and 4; ΔG^{298} between −15.5 and −81.7 kJ•mol^{-1}) indicating an additional stabilisation of the final products by the water molecules. Thus, for primary amines the water is not changing the ability of the amines to capture CO_2 from the gas phase. This is in good agreement with the adsorption results because no noticeable effects on the equilibrium curves obtained in dry and humid conditions are observed. For the tertiary amine (DEAPTES@SBA-15), the reaction of CO_2 is clearly unfavourable ($\Delta G^{298} = \sim 230$ kJ•mol^{-1}). The calculations with this model were challenging because when the CO_2 is removed

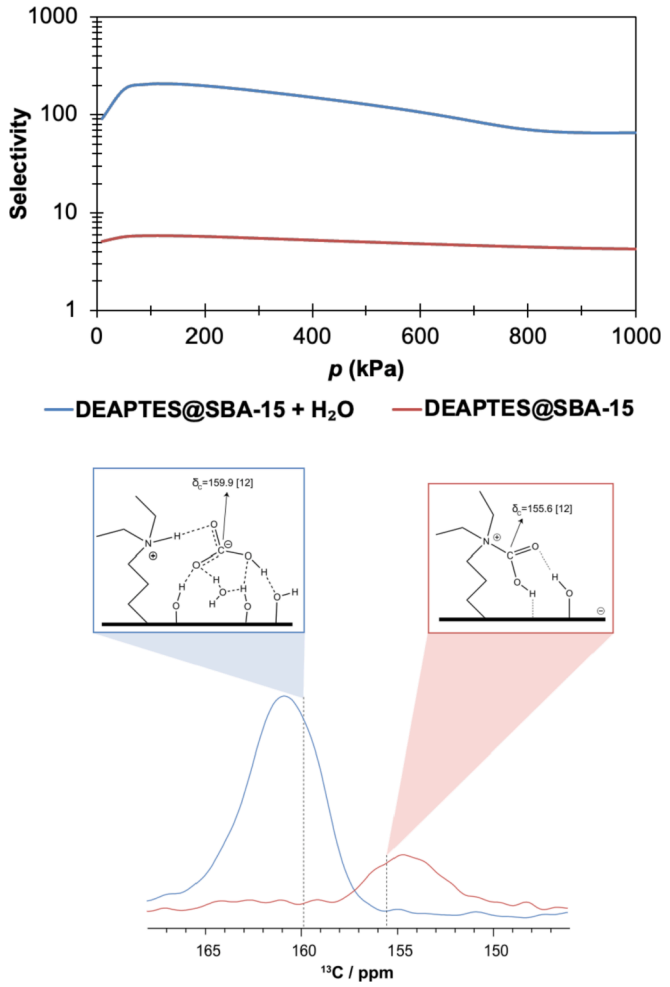

Fig. 4. Variation of the average selectivity towards CO_2 at 25 °C and up to 1000 kPa, and corresponding NMR spectra of samples with adsorbed $^{13}CO_2$ and DEAPTES@SBA-15 under dry (red lines) and wet (blue lines) conditions. The assignment of the chemical shifts (in ppm) to the corresponding structures was assisted by DFT calculations on cluster models and the details are given in the references above the structures. The highest amount of pre-adsorbed water vapour was considered for DEAPTES@SBA-15. The average selectivity was determined using the data obtained with 0.140 mmol•g^{-1} and 0.133 mmol•g^{-1} of pre-adsorbed water vapour, for the adsorption of CO_2 and CH_4, respectively (*cf.* Fig. 2 and Table 2).

from the initial model, the integrity of the resulting structure is damaged by decomposition reactions that lead to loss of crystallinity, clearly supportive of an extremely unstable structure. In contrast, the presence of water makes the reaction of the tertiary amine with CO_2 highly favoured (ΔG^{298} = -24.3 kJ•mol^{-1}) since the final product of the reaction is different. As above-mentioned, water also reacts during this process to produce a bicarbonate species that is stable, as evidenced by NMR. Encouragingly, the overall results in Table 3 agree with the changes observed on the phase diagrams for DEAPTES@SBA-15 (Fig. 5b). The experimental and computational results were obtained at 25 °C, but industrial application of adsorbent in adsorption columns are normally subjected to considerable temperature fluctuations, even in PSA operations, due to the exothermic nature of adsorption. However, the working temperature of 25 °C is representative of a feed gas temperature; it is expected that the column temperature should oscillate around this value during the adsorption/desorption cycles. Thus, the phase diagrams and calculated energies are a first good indication of the expected behaviour of the materials in columns.

Considering an initial biogas feed with traces of water, during a first cycle of a PSA-type separation using DEAPTES@SBA-15, the relative amount of water (regarding CO_2) already present in the feed, would not be sufficiently high to induce the increase in CO_2 uptake due to the formation of bicarbonate. In this case, the competitive adsorption of the much higher amounts of CO_2 in the gas stream would leave fewer active sites available for the water molecules to bind to [12]. This would effectively result in a situation analogous to that observed for the adsorption of CO_2 under dry conditions. After the first adsorption cycle, the regeneration of the material (by depressurisation of the adsorption column) would remove the adsorbed CO_2 species (and CH_4, albeit in a much lower quantity), leaving the strongly adsorbed water molecules on the pore surface of the material. From the second separation cycle onwards, "pre-adsorbed" water remains on the pore surface of the material, and the results would be analogous to those observed under wet conditions for DEAPTES@SBA-15 in this work, *i.e.*, there would be a considerable increase in CO_2 uptake and a tremendous enhancement of the CO_2/CH_4 separation selectivity.

4. Conclusions

Primary- and tertiary-amine-modified mesoporous silicas (APTES@SBA-15 and DEAPTES@SBA-15) have been studied for the adsorption of CO_2 and CH_4 under dry and wet conditions. These adsorbent materials present a much higher CO_2 uptake than CH_4, which is a good indicator of their potential for CO_2/CH_4 separation. Under dry conditions, APTES@SBA-15 has a higher CO_2 uptake than DEAPTES@SBA-15, mainly resulting from the type and strength of the interactions involving primary amines reacting with CO_2 at the pore surface. For APTES@SBA-15, results have shown that the presence of small amounts of pre-adsorbed water (<0.15 mmol•g^{-1}) does not significantly affect the adsorption of CO_2 and CH_4. For DEAPTES@SBA-15 there is a notable increase in CO_2 uptake in the presence of pre-adsorbed water: the results from the sample with the highest amount of water (*ca.* 0.140 mmol•g^{-1}) are, on average (over the whole pressure range studied), twice as high as on the dry material. This significant increase has been attributed to the formation of bicarbonate species under wet conditions, which is absent in primary amines as evidenced by NMR spectroscopy. Indeed, the presence of bicarbonate leads to a significant increase in the selectivity for CO_2 in the CO_2/CH_4 separation for DEAPTES@SBA-15 (maximum selectivity under dry and wet conditions is, respectively, *ca.* 5.8 and 208), showing the remarkable effect of pre-adsorbed water on the separation process using tertiary amines. Conversely, the presence of small amounts of water in the primary amine material (APTES@SBA-15) did not significantly change the selectivity or phase equilibrium in comparison with the dry counterpart.

The different adsorption behaviour between primary and tertiary amine-grafted adsorbents was correlated with the significant differences in the NMR spectra of the samples loaded with $^{13}CO_2$ in dry and wet samples. DFT calculations employing the models that describe the experimental ^{13}C chemical shifts confirmed that there is a change in the type of reaction of the tertiary amine under moist conditions (*i.e.* formation of bicarbonate with water as a reactant). In the case of primary amines, there is essentially an overall stabilisation of the final products by the presence of water.

We have shown that the presence of residual amounts of pre-adsorbed water on the pore surface of silicas functionalised with tertiary amines induces a tremendous effect on the separation of CO_2 and CH_4 in adsorption-based processes. In a typical biogas stream undergoing purification via PSA-type processes using this type of material, the low amounts of water present in the feed would not induce any effect on the separation of CO_2 and CH_4 during the first adsorption cycle, due to the competitive adsorption of the much higher amounts of CO_2. However, the depressurisation of the column, performed on the first regeneration, would not remove the water molecules adsorbed onto the pore surface, which would potentially lead to the effects observed in the scope of this work in the ensuing separation cycles.

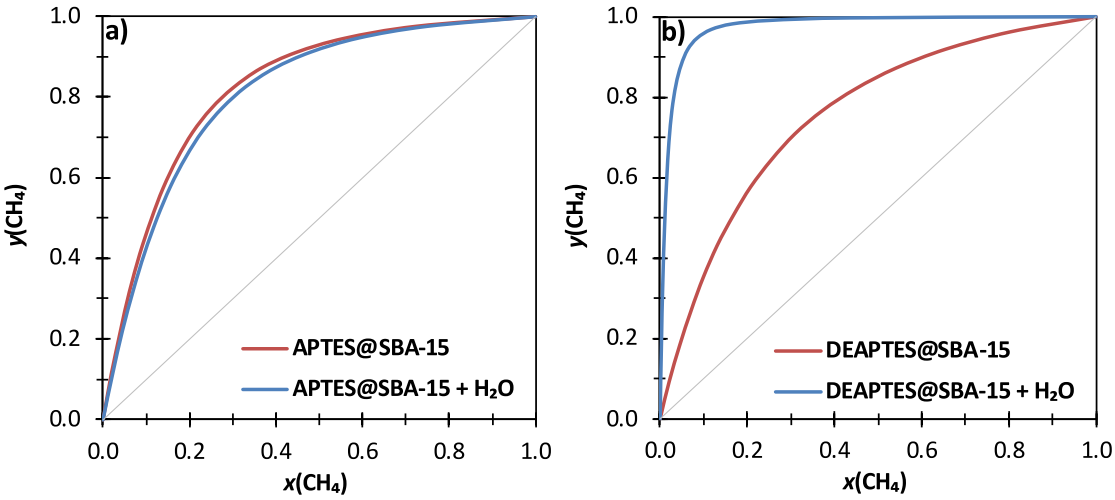

Fig. 5. Isothermal (25 °C), isobaric (500 kPa) *xy* phase diagram for the adsorption of CO_2/CH_4 mixtures on APTES@SBA-15 (a) and DEAPTES@SBA-15 (b) under dry (red) and wet (blue) conditions. The highest amount of pre-adsorbed water vapour was considered for each material and gas under wet conditions, so that for DEAPTES@SBA-15, the phase diagram was determined using the data obtained with 0.140 mmol•g^{-1} and 0.133 mmol•g^{-1} of pre-adsorbed water vapour, for the adsorption of CO_2 and CH_4, respectively (*cf.* Fig. 2 and Table 2). $y(CH_4)$ and $x(CH_4)$ represent the molar fractions of methane in the gas and adsorbed phases, respectively.

Table 3
Reaction Gibbs energies of CO_2 with the primary amine (APTES), and tertiary amine (3-DEPATES) estimated by computational methods (see text and Figs. 3 and 4 for corresponding structures). Note: values marked with * were calculated using an initial reference structure (without CO_2) slightly more stable than previously reported.

Material		ΔE^o	ΔG^{298}	Calculated ^{13}C chemical shift
		kJ•mol^{-1}	kJ•mol^{-1}	ppm
APTES@SBA-15	Dry	−51.9	−7.1 [10]	160.2 [11]
		−33.9	8.9* −5.6 [10]	162.9 [11]
		−93.0	−43.3	163.7 [12]
		−32.1	9.8* −4.7 [10]	154.0 [11]
	Wet	−188.5	−81.7	166.0 [12]
		−64.4	−15.5	161.0 [11]
DEAPTES@SBA-15				
	Dry	151.6	230.2	155.6 [12]
	Wet	−73.4	−24.3	159.9 [12]

Declaration of Competing Interest

The authors declare that they have no known competing financial interests or personal relationships that could have appeared to influence the work reported in this paper.

Acknowledgements

This work was developed in the scope of project CICECO-Aveiro Institute of Materials from the University of Aveiro ref. UIDB/50011/2020 & UIDP/50011/2020, project CERENA ref. UIDB/04028/2020 & UIDP/04028/2020. We also acknowledge funding from projects ref. PTDC/QUI-QFI/28747/2017 (GAS2MATDNPSENS - POCI-01-0145-FEDER-028747), PTDC/QUI-QFI/31002/2017 (SILVIA - CENTRO-01-0145-FEDER-31002), PTDC/QEQ-QAN/6373/2014 and Smart Green Homes POCI-01-0247-FEDER-007678, a co-promotion between Bosch Termotecnologia S.A. and the University of Aveiro. These projects are financed through FCT/MEC and co-financed by FEDER under the PT2020 Partnership Agreement. The NMR spectrometers are part of the National NMR Network (PTNMR) and are partially supported by Infrastructure Project 022161 (co-financed by FEDER through COMPETE 2020, POCI and PORL and FCT through PIDDAC). This work has received funding from the European Research Council (ERC) under the European Union's Horizon 2020 research and innovation programme (grant agreement no. 865974). MS would also like to thank FCT for the individual CEEC contract (2020.00056.CEECIND).

Appendix A. Supplementary data

Supporting information file with infrared and ^{13}C ssNMR spectra, and thermogravimetric analysis of the samples. Supplementary data to this article can be found online at https://doi.org/10.1016/j.cej.2022.136271.

References

[1] J.I. Huertas, N. Giraldo, S. Izquierdo, Removal of H2S and CO2 from biogas by amine absorption, Mass Transf. Chem. Eng. Process. (2011), https://doi.org/10.5772/20039.
[2] M. Bui, C.S. Adjiman, A. Bardow, E.J. Anthony, A. Boston, S. Brown, P.S. Fennell, S. Fuss, A. Galindo, L.A. Hackett, J.P. Hallett, H.J. Herzog, G. Jackson, J. Kemper, S. Krevor, G.C. Maitland, M. Matuszewski, I.S. Metcalfe, C. Petit, G. Puxty, J. Reimer, D.M. Reiner, E.S. Rubin, S.A. Scott, N. Shah, B. Smit, J.P.M. Trusler, P. Webley, J. Wilcox, N. Mac Dowell, Carbon capture and storage (CCS): The way forward, Energy Environ. Sci. 11 (2018) 1062–1176, https://doi.org/10.1039/c7ee02342a.
[3] E.I. Koytsoumpa, C. Bergins, E. Kakaras, The CO2 economy: Review of CO2 capture and reuse technologies, J. Supercrit. Fluids. 132 (2018) 3–16, https://doi.org/10.1016/j.supflu.2017.07.029.
[4] G. Singh, J. Lee, A. Karakoti, R. Bahadur, J. Yi, D. Zhao, K. AlBahily, A. Vinu, Emerging trends in porous materials for CO2 capture and conversion, Chem. Soc. Rev. 49 (13) (2020) 4360–4404.
[5] E.S. Sanz-Pérez, C.R. Murdock, S.A. Didas, C.W. Jones, Direct Capture of CO2 from Ambient Air, Chem. Rev. 116 (2016) 11840–11876, https://doi.org/10.1021/acs.chemrev.6b00173.
[6] P. Bollini, S.A. Didas, C.W. Jones, Amine-oxide hybrid materials for acid gas separations, J. Mater. Chem. 21 (2011) 15100–15120, https://doi.org/10.1039/c1jm12522b.
[7] N. Hiyoshi, K. Yogo, T. Yashima, Adsorption of carbon dioxide on amine modified SBA-15 in the presence of water vapor, Chem. Lett. 33 (2004) 510–511, https://doi.org/10.1246/cl.2004.510.
[8] X. Xu, C. Song, B.G. Miller, A.W. Scaroni, Influence of Moisture on CO2 Separation from Gas Mixture by a Nanoporous Adsorbent Based on Polyethylenimine-Modified Molecular Sieve MCM-41, Ind. Eng. Chem. Res. 44 (2005) 8113–8119, https://doi.org/10.1021/ie050382n.
[9] A.D. Ebner, M.L. Gray, N.G. Chisholm, Q.T. Black, D.D. Mumford, M.A. Nicholson, J.A. Ritter, Suitability of a solid amine sorbent for CO2 capture by pressure swing adsorption, Ind. Eng. Chem. Res. 50 (2011) 5634–5641, https://doi.org/10.1021/ie2000709.

[10] L. Mafra, T. Čendak, S. Schneider, P.V. Wiper, J. Pires, J.R.B. Gomes, M.L. Pinto, Amine functionalized porous silica for CO2/CH4 separation by adsorption: Which amine and why, Chem. Eng. J. 336 (2018) 612–621, https://doi.org/10.1016/j.cej.2017.12.061.
[11] L. Mafra, T. Čendak, S. Schneider, P.V. Wiper, J. Pires, J.R.B. Gomes, M.L. Pinto, Structure of Chemisorbed CO2 Species in Amine-Functionalized Mesoporous Silicas Studied by Solid-State NMR and Computer Modeling, J. Am. Chem. Soc. 139 (2017) 389–408, https://doi.org/10.1021/jacs.6b11081.
[12] M. Sardo, R. Afonso, J. Juźków, M. Pacheco, M. Bordonhos, M.L. Pinto, J.R. B. Gomes, L. Mafra, Unravelling moisture-induced CO2 chemisorption mechanisms in amine-modified sorbents at the molecular scale, J. Mater. Chem. A. 9 (2021) 5542–5555, https://doi.org/10.1039/d0ta09808f.
[13] J. Rouquerol, F. Rouquerol, K. Sing, Adsorption by Powders and Porous Solids: Principles, Methodology and Applications, 1st ed., Academic Press, San Diego, 1999.
[14] W.W. Lukens, P. Schmidt-Winkel, D. Zhao, J. Feng, G.D. Stucky, Evaluating pore sizes in mesoporous materials: a simplified standard adsorption method and a simplified Broekhoff-de Boer method, Langmuir 15 (1999) 5403–5409, https://doi.org/10.1021/la990209u.
[15] J. Pires, A. Carvalho, M. Pinto, J. Rocha, Characterization of Y zeolites dealuminated by solid-state reaction with ammonium hexafluorosilicate, J. Porous Mater. 13 (2006) 107–114, https://doi.org/10.1007/s10934-006-7005-x.
[16] M. Bordonhos, M. Lourenço, J.R.B. Gomes, P. Ferreira, M.L. Pinto, Exploring periodic mesoporous organosilicas for ethane–ethylene adsorption–separation, Microporous Mesoporous Mater. 317 (2021), 110975, https://doi.org/10.1016/j.micromeso.2021.110975.
[17] A.L. Myers, P.A. Monson, Adsorption in porous materials at high pressure: Theory and experiment, Langmuir 18 (2002) 10261–10273, https://doi.org/10.1021/la026399h.
[18] A.L. Myers, Equation of State for Adsorption of Gases and Their Mixtures in Porous Materials, Adsorption. 9 (2003) 9–16, https://doi.org/10.1023/A:1023807128914.
[19] A.L. Myers, J.M. Prausnitz, Thermodynamics of Mixed-Gas Adsorption, AIChE J. 11 (1965) 121–127, https://doi.org/10.1002/aic.690110125.
[20] M.L. Pinto, J. Pires, J. Rocha, Porous Materials Prepared from Clays for the Upgrade of Landfill Gas, J. Phys. Chem. C. 112 (2008) 14394–14402, https://doi.org/10.1021/jp803015d.
[21] J. Pires, V.K. Saini, M.L. Pinto, Studies on Selective Adsorption of Biogas Components on Pillared Clays: Approach for Biogas Improvement, Environ. Sci. Technol. 42 (2008) 8727–8732, https://doi.org/10.1021/es8014666.
[22] Y. Zhao, D.G. Truhlar, The M06 suite of density functionals for main group thermochemistry, thermochemical kinetics, noncovalent interactions, excited states, and transition elements: Two new functionals and systematic testing of four M06-class functionals and 12 other function, Theor. Chem. Acc. 120 (2008) 215–241, https://doi.org/10.1007/s00214-007-0310-x.
[23] Y. Zhao, D.G. Truhlar, Comparative DFT study of van der Waals complexes: Rare-gas dimers, alkaline-earth dimers, zinc dimer and zinc-rare-gas dimers, J. Phys. Chem. A. 110 (2006) 5121–5129, https://doi.org/10.1021/jp060231d.
[24] P.C. Hariharan, J.A. Pople, The influence of polarization functions on molecular orbital hydrogenation energies, Theor. Chim. Acta. 28 (1973) 213–222, https://doi.org/10.1007/BF00533485.
[25] M.M. Francl, W.J. Pietro, W.J. Hehre, J.S. Binkley, M.S. Gordon, D.J. DeFrees, J. A. Pople, Self-consistent molecular orbital methods. XXIII. A polarization-type basis set for second-row elements, J. Chem. Phys. 77 (1982) 3654–3665, https://doi.org/10.1063/1.444267.
[26] M.J. Frisch, G.W. Trucks, H.B. Schlegel, G.E. Scuseria, M.A. Robb, J.R. Cheeseman, G. Scalmani, V. Barone, B. Mennucci, G.A. Petersson, H. Nakatsuji, M. Caricato, X. Li, H.P. Hratchian, A.F. Izmaylov, J. Bloino, G. Zheng, J.L. Sonnenberg, M. Hada, M. Ehara, K. Toyota, R. Fukuda, J. Hasegawa, M. Ishida, T. Nakajima, Y. Honda, O. Kitao, H. Nakai, T. Vreven, J.A. Jr., J.E. Peralta, F. Ogliaro, M. Bearpark, J.J. Heyd, E. Brothers, K.N. Kudin, V.N. Staroverov, T. Keith, R. Kobayashi, J. Normand, K. Raghavachari, A. Rendell, J.C. Burant, S.S. Iyengar, J. Tomasi, M. Cossi, N. Rega, J. M. Millam, M. Klene, J.E. Knox, J.B. Cross, V. Bakken, C. Adamo, J. Jaramillo, R. Gomperts, R.E. Stratmann, O. Yazyev, A.J. Austin, R. Cammi, C. Pomelli, J.W. Ochterski, R.L. Martin, K. Morokuma, V.G. Zakrzewski, G.A. Voth, P. Salvador, J.J. Dannenberg, S. Dapprich, A.D. Daniels, O. Farkas, J.B. Foresman, J. V. Ortiz, J. Cioslowski, D.J. Fox, Gaussian 09, Revision B.01, Gaussian, Inc., Wallingford CT, (2010).
[27] R. Afonso, M. Sardo, L. Mafra, J.R.B. Gomes, Unravelling the Structure of Chemisorbed CO2 Species in Mesoporous Aminosilicas: A Critical Survey, Environ. Sci. Technol. 53 (2019) 2758–2767, https://doi.org/10.1021/acs.est.8b05978.
[28] K. Wolinski, J.F. Hinton, P. Pulay, Efficient Implementation of the Gauge-Independent Atomic Orbital Method for NMR Chemical Shift Calculations, J. Am. Chem. Soc. 112 (1990) 8251–8260, https://doi.org/10.1021/ja00179a005.
[29] J.R. Cheeseman, G.W. Trucks, T.A. Keith, M.J. Frisch, A comparison of models for calculating nuclear magnetic resonance shielding tensors, J. Chem. Phys. 104 (1996) 5497–5509, https://doi.org/10.1063/1.471789.
[30] T. Čendak, L. Sequeira, M. Sardo, A. Valente, M.L. Pinto, L. Mafra, Detecting Proton Transfer in CO2 Species Chemisorbed on Amine-Modified Mesoporous Silicas by Using 13C NMR Chemical Shift Anisotropy and Smart Control of Amine Surface Density, Chem. - A Eur. J. 24 (2018) 1–11, https://doi.org/10.1002/chem.201800930.
[31] A. Sayari, Y. Belmabkhout, Stabilization of Amine-Containing CO2 Adsorbents: Dramatic Effect of Water Vapor, J. Am. Chem. Soc. 132 (2010) 6312–6314, https://doi.org/10.1021/ja1013773.
[32] S.A. Didas, M.A. Sakwa-Novak, G.S. Foo, C. Sievers, C.W. Jones, Effect of Amine Surface Coverage on the Co-Adsorption of CO2 and Water: Spectral Deconvolution of Adsorbed Species, J. Phys. Chem. Lett. 5 (2014) 4194–4200, https://doi.org/10.1021/jz502032c.
[33] R. Serna-Guerrero, E. Da'na, A. Sayari, New Insights into the Interactions of CO2 with Amine-Functionalized Silica, Ind. Eng. Chem. Res. 47 (23) (2008) 9406–9412.